S1. Calibration of NO_2 monitors

Three cavity attenuated phase-shift spectrometry (CAPS) instruments (Aerodyne Research) were used for measuring NO_2 (Kebabian et al., 2008;Kebabian et al., 2005). Two were dedicated for the measurements of NO_2 as part of the ECHAMP measurement of peroxy radicals. The third CAPS instrument was used for measuring ambient NO_2. The NO_2 monitors were calibrated by sampling diluted NO_2(g) from a liquid permeation tube (Kin-Tek). The output of the permeation tube (held at 40° C) was diluted into 100 sccm of N_2 and then into variable flow rates (4000 to 8000 sccm) of either zero air or purified ambient air to make multiple points in the calibration curve. The purified ambient air was prepared by passing ambient air through a scrubber filled with sodium permanganate and activated charcoal (Purafil brand SP Blend Media). The concentrations of NO_2 delivered from the permeation tube were quantified by a chemiluminescence analyzer (Model 42i Trace Level, Thermo Scientific) where the NO_2 was converted to NO (NO_x mode) in a molybdenum converter held at 325 °C. See section 3 below for chemiluminescence sensor calibration information. The CAPS NO_2 measurements were also checked by comparing the ECHAMP readings when in "Ox" (background) mode to measurements of O_3 by a UV-absorption monitor (2B Tech model 202, accuracy 2%). The two methods agreed to within 5% (Wood and Charest, 2014).

S2. ECHAMP calibration

The ECHAMP sensor was calibrated using the acetone photolysis method (Wood and Charest, 2014). Photolysis of acetone vapor produces almost equimolar concentrations of methyl peroxy (CH_3O_2) and peroxyacetyl ($CH_3C(O)OO$) radicals:

$$CH_3C(O)CH_3 + h\nu\ (254\ nm) + 2O_2 \rightarrow CH_3O_2 + CH_3C(O)OO \quad (S1)$$

Following reaction with excess NO, these RO_2 radicals will produce NO_2 via the following reactions:

$$CH_3C(O)OO + NO \rightarrow CH_3C(O)O + NO_2 \quad (S2)$$
$$CH_3C(O)O + M + O_2 \rightarrow CH_3O_2 + CO_2 + M \quad (S3)$$
$$CH_3O_2 + NO \rightarrow CH_3O + NO_2 \quad (S4)$$
$$CH_3O + O_2 \rightarrow HO_2 + HCHO \quad (S5a)$$
$$CH_3O + NO + M \rightarrow CH_3ONO + M \quad (S5b)$$
$$HO_2 + NO \rightarrow OH + NO_2 \quad (S6)$$

Ignoring the formation of methyl nitrite (Reaction S5b), each CH_3O_2 radical would produce two NO_2 molecules and each $CH_3C(O)OO$ would produce three NO_2 molecules. The change in NO_2 observed when the radical source is modulated on and off, effected by diverting the acetone flow away from the carrier flow that is illuminated by the UV source, is related to the RO_2 concentration by the following equation:

$$([CH_3O_2] + [CH_3C(O)OO]) = \Delta NO_2 / (2.44 \times 0.95) \quad (S7)$$

in the absence of CH_3ONO formation and if acetone photolysis at 254 nm led to CH_3O_2 and $CH_3C(O)O_2$ with unity photolysis quantum yield, then the denominator of the right-hand side of

the equation would be exactly 2.5. The two factors in the denominator account for these two processes as described in Wood and Charest (2014).

As described in the main text, during the field July 2015 field deployment we produced acetone vapor by flowing air over the headspace of dilute aqueous acetone rather than over pure acetone. Unfortunately this produced variable amounts of blue light-absorbing compounds (possibly glyoxal, methyl glyoxal, or diacetyl) which interfered with the CAPS detection of NO_2. As a result we relied on laboratory calibrations performed in the laboratory rather than in-field calibrations (Fig S1).

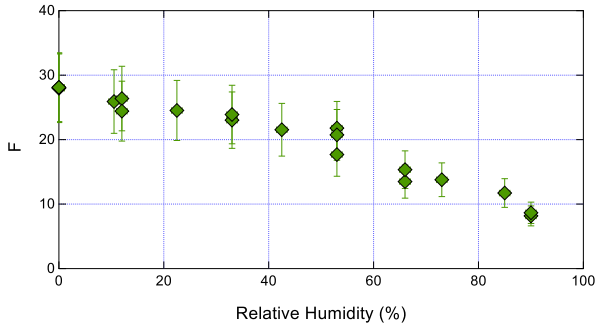

Fig. S1. Amplification factors obtained for ECHAMP using the acetone photolysis method. Uncertainty bars reflect the 2σ accuracy of 19%.

S3. Sampling losses in the ECHAMP inlet.

Sampled air flowed through a glass cross that is internally coated with halocarbon wax and into the two FEP/PFA reaction chambers, both of which comprise a ¼" PFA tee and ¼" OD, 0.156" (0.4 cm) ID FEP tubing. The total residence time in the cross was approximately 18 ms. We quantified potential sampling losses in the cross in two ways – 1. by quantifying the effective first order wall loss rate constant of HO_2 and isoprene peroxy radicals onto halocarbon wax-coated glass of the same dimensions, and 2. by comparing the ECHAMP signal when an HO_2 source was used to overflow the sampling cross and comparing to the signal when the HO_2 source directly overflowed one of the reaction chambers (at the PFA tee).

The wall loss rate constant measurements for several types of material will be fully described in a separate manuscript. Briefly, peroxy radicals were produced by illumination of humidified air (8 – 10 LPM) by UV radiation from a mercury lamp:

$$H_2O + O_2 + UV\ (185\ nm) \rightarrow HO_2 + OH \qquad (S8)$$

A 50 sccm flow of 0.1% CO was added to convert all OH into HO_2. Similarly, adding 50 sccm of isoprene (40 ppm, balance N_2) to the flow converted all OH into isoprene peroxy radicals,

producing a mixture of 50% HO_2 and 50% isoprene peroxy radicals. This source was used to overflow a quartz tube internally coated with halocarbon wax connected to the sampling cross, and the transmitted radicals were quantified by ECHAMP. Four different lengths of tubing were used: 147 cm, 86", 25", and 0" (i.e., no tube).

The loss rate constants increased with RH, and at 60% RH were $1.6 \pm 0.6\ s^{-1}$ for HO_2 and approximately 0.9 for HO_2/isopreneRO$_2$, indicating lower losses for isoprene RO_2 than for HO_2. This suggests losses of HO_2 were only 3% during the 18 ms sampling time. Losses of CH_3O_2 radicals were similarly investigated and showed negligible losses (< 1%) onto halocarbon wax and other fluoropolymers for sampling times under 1 second.

Similarly, the second method – comparing the ECHAMP signal when sampling a radical source through the sampling cross or directly into one of the reaction chambers – indicated overall losses of less than 4% for an HO_2 source.

S4. Calibration of NO chemiluminescence monitor.

The Thermo 42i-TL chemiluminescence monitor was calibrated by dilution of gas from a 30 ppm NO standard cylinder with zero grad air using MKS brand mass flow controllers (model 1179A). The flow rates from these flow controllers agreed to within 1% when measured by separately calibrated flow meters (Definer 220, BIOS/Mesa Labs). The humidity dependence of the chemiluminescence sensor was determined by humidification of the diluent zero air.

S5. Baseline measurements for NO, NO_2, and O_3 measurements.

Baseline (zero) measurements were executed every 10 minutes for the NO, NO_2, and O_3 measurements by overflowing their common inlet with purified air. This air was prepared by drawing outdoor air sequentially through a PTFE filter, a diaphragm pump, 800 cm^3 of $KMnO_4$(s), 600 cm^3 of a blend of $KMnO_4$ and activated charcoal, and finally a second PTFE filter.

S6. Calculated Ozone Production Rates

Net formation of ozone occurs when peroxy radicals oxidize NO to NO_2, followed by photolysis of NO_2 (Seinfeld and Pandis, 2012;Finlayson-Pitts and Pitts Jr, 1999;Haagen-Smit et al., 1954). Therefore, the instantaneous gross O_3 production rate (or more accurately, O_X production rate where $[O_X] \equiv [O_3] + [NO_2]$) can be calculated by the following equation:

$$P(O_3) = k_{XO_2+NO}[XO_2][NO] \quad \text{(S9)}$$

where k_{XO2+NO} is a weighted rate constant for the reaction of the various peroxy radicals with NO. $P(O_3)$ measurements are useful for assessing the temporal profile of ozone production, help to quantify local production versus transport, and can identify the chemical regime (NOx-limited vs. NOx-saturated) of an air mass. We use a value of 9×10^{-12} cm^3 $molecule^{-1}$ s^{-1} for the value of k, reflecting a reasonable assumption that isoprene peroxy radicals and HO_2 had large contributions to the total peroxy radical concentration. These two peroxy radicals react with NO with rate constants of 9×10^{-12} cm^3 $molecule^{-1}$ s^{-1} and 8.8×10^{-12} cm^3 $molecule^{-1}$ s^{-1}, respectively (Atkinson et al., 2004;Sander et al., 2006). We note that the chemical amplification technique does not detect the portion of organic peroxy radicals that form organic nitrates ($RONO_2$) upon reaction with NO; thus no correction for organic nitrate yields are needed in equation 2.

$P(O_3)$ values calculated based on 15-min average concentrations of the related chemical species are shown in Fig. S1 along with XO_2 radicals, O_3 and NO during the IRRONIC campaign over the time period of 16 July - 25 July. The missing $P(O_3)$ data on Fig. 6 are due to unavailability of either NO or XO_2 measurements due to calibrations or technical problems with the chemiluminescence instrument. 15-min average $P(O_3)$ values between 9:00 and 21:00 were at most 9.4 ppb hr^{-1}, with significant inter-day variability. For example $P(O_3)$ exceeded 7.0 ppb/hr for several hours on 18 July but never exceeded 5.0 ppb/hr on 22 or 16 July. Peak $P(O_3)$ values occurred between 9 and 11 am, with average values between 3.3 and 7.8 ppb hr^{-1}.

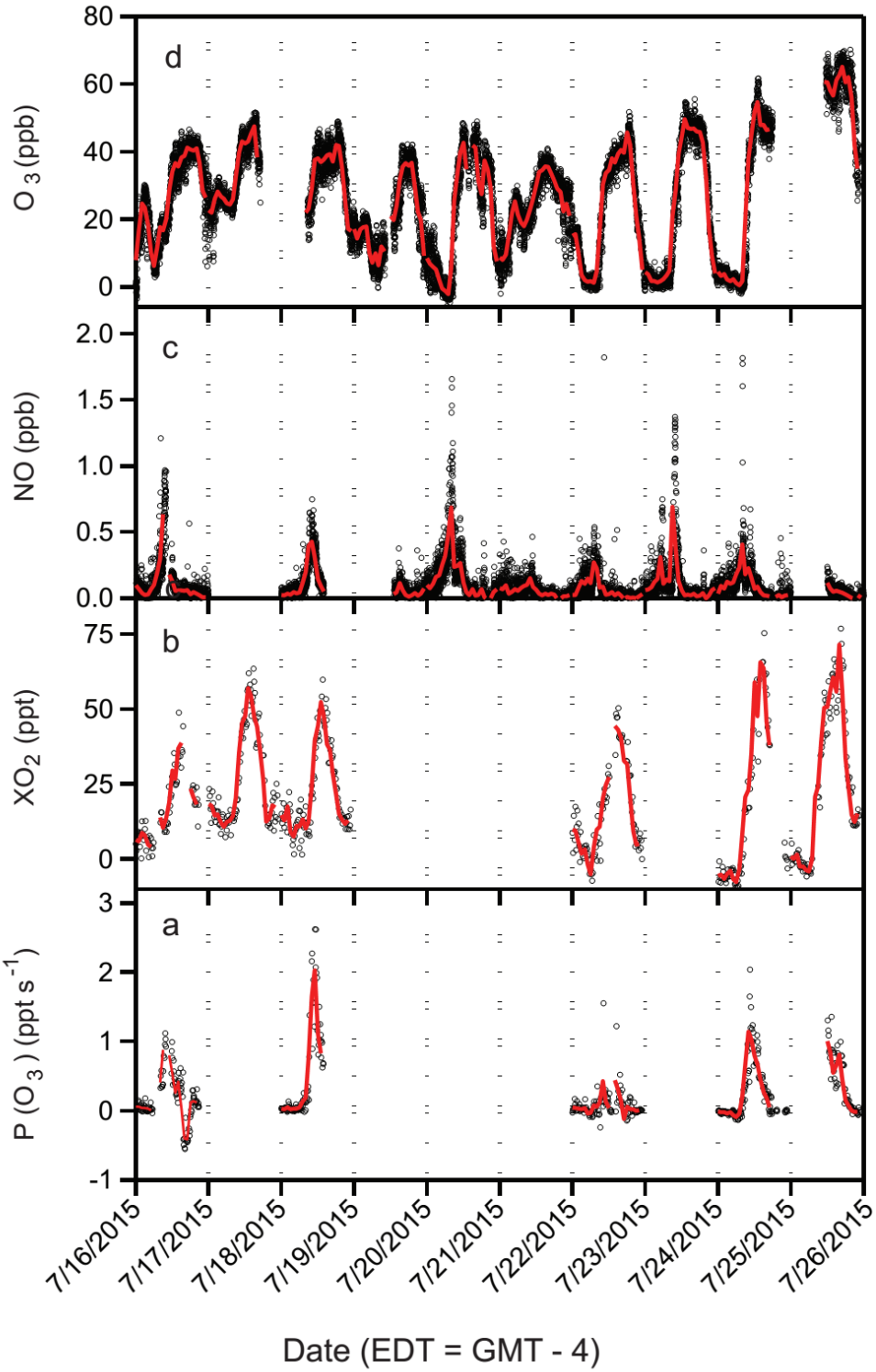

Fig S2. Temporal variations of a) calculated ozone production rate ($P(O_3)$), b) total peroxy radicals (XO_2), c) NO and d) O_3 during the IRRONIC campaign over the time period of 16 July to 25 July. The missing values of $P(O_3)$ are related with the unavailability of either XO_2 or NO measurements.

The observed $P(O_3)$ values at our study site are in general lower than those observed in urban areas, which have exceeded 50 ppb h^{-1} in Mexico City and Houston (Cazorla et al., 2012;Kleinman et al., 2005;Shirley et al., 2006). The main reason is that both the NO concentrations and primary HOx production rates (from $O(^1D) + H_2O$ and the photolysis of HONO and oxygenated VOCs) were significantly lower during the IRRONIC campaign compared to those reported in the mentioned urban areas. $P(O_3)$ was highest in the late morning (9 – 11 am) when NO was highest as well. The overall positive correlation between $P(O_3)$ and [NO] suggests that ozone production regime was almost always NO_x-limited (see Fig. S2).

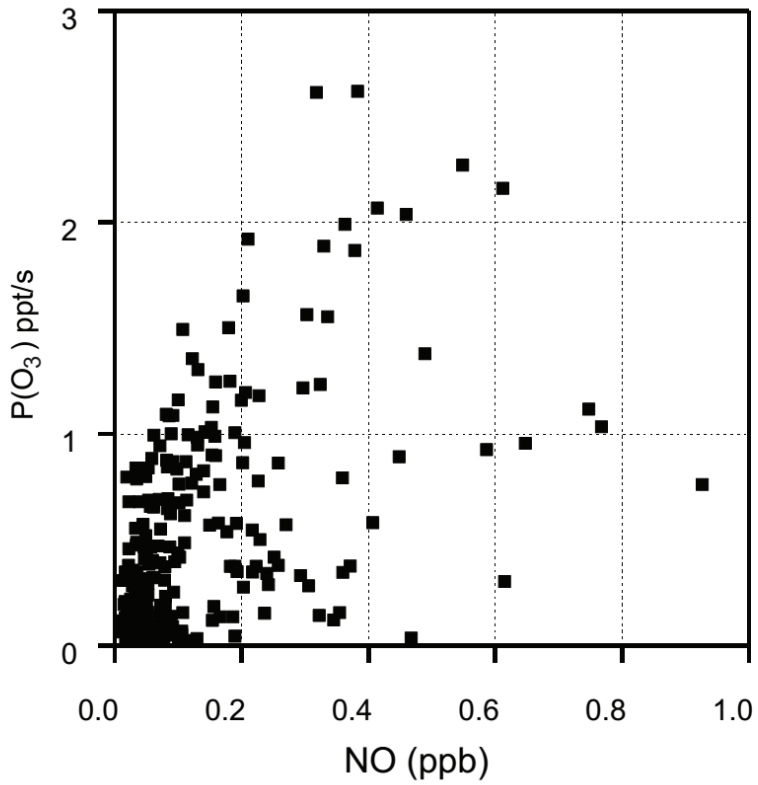

Fig. S3. Relationship between $P(O_3)$ and NO during the daytime (09:00 to 21:00) over the time period of 13-25 July.

S6. Comparison of Peroxy radical speciation predicted by RACM2, RACM2-LIM1, MCM 3.2, and MCM 3.3.1

The four figures below show the diurnal average composition of peroxy radicals as predicted by the four chemical mechanisms.

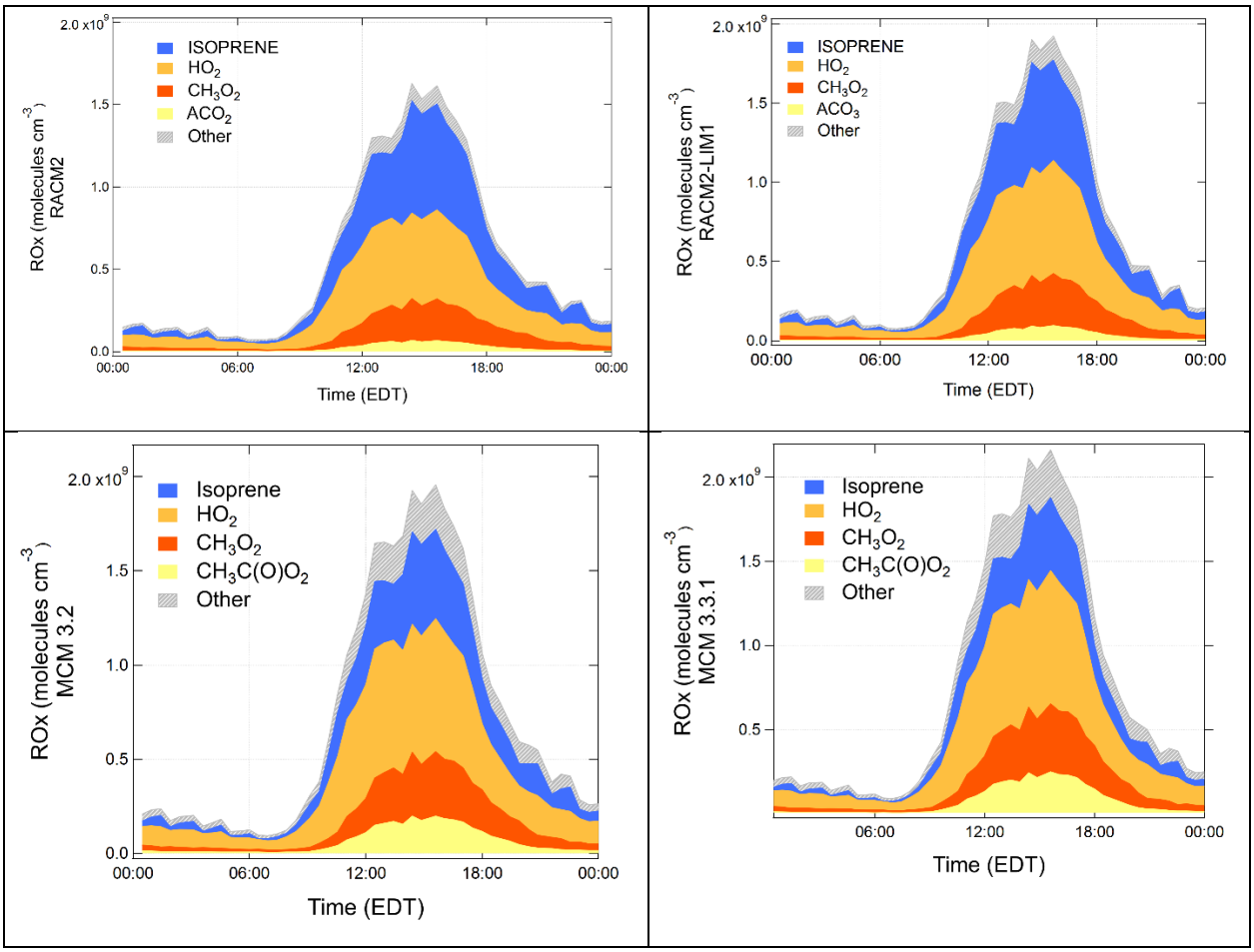

Fig S4. Diurnal profile of peroxy radical concentrations predicted by the four chemical mechanisms

References:

Atkinson, R., Baulch, D., Cox, R., Crowley, J., Hampson, R., Hynes, R., Jenkin, M., Rossi, M., and Troe, J.: Evaluated kinetic and photochemical data for atmospheric chemistry: Volume I-gas phase reactions of O x, HO x, NO x and SO x species, Atmos Chem Phys, 4, 1461-1738, 2004.

Cazorla, M., Brune, W. H., Ren, X., and Lefer, B.: Direct measurement of ozone production rates in Houston in 2009 and comparison with two estimation methods, Atmos. Chem. Phys., 12, 1203-1212, 10.5194/acp-12-1203-2012, 2012.

Finlayson-Pitts, B. J., and Pitts Jr, J. N.: Chemistry of the upper and lower atmosphere: theory, experiments, and applications, Academic press, 1999.

Haagen-Smit, A., Bradley, C., and Fox, M.: Ozone Formation in Photochemical Oxidation of Organic Substances, Rubber Chemistry and Technology, 27, 192-200, 1954.

Kebabian, P. L., Herndon, S. C., and Freedman, A.: Detection of Nitrogen Dioxide by Cavity Attenuated Phase Shift Spectroscopy, Analytical Chemistry, 77, 724-728, 10.1021/ac048715y, 2005.

Kebabian, P. L., Wood, E. C., Herndon, S. C., and Freedman, A.: A practical alternative to chemiluminescence-based detection of nitrogen dioxide: cavity attenuated phase shift spectroscopy, Environmental science & technology, 42, 6040-6045, 2008.

Kleinman, L. I., Daum, P. H., Lee, Y. N., Nunnermacker, L. J., Springston, S. R., Weinstein-Lloyd, J., and Rudolph, J.: A comparative study of ozone production in five U.S. metropolitan areas, Journal of Geophysical Research-Atmospheres, 110, doi:10.1029/2004JD005096, 2005.

Sander, S. P., Friedl, R., Golden, D., Kurylo, M., Moortgat, G., Wine, P., Ravishankara, A., Kolb, C., Molina, M., and Finlayson-Pitts, B.: Chemical kinetics and photochemical data for use in atmospheric studies evaluation number 15, 2006.

Seinfeld, J. H., and Pandis, S. N.: Atmospheric chemistry and physics: from air pollution to climate change, John Wiley & Sons, 2012.

Shirley, T. R., Brune, W. H., Ren, X., Mao, J., Lesher, R., Cardenas, B., Volkamer, R., Molina, L. T., Molina, M. J., Lamb, B., Velasco, E., Jobson, T., and Alexander, M.: Atmospheric oxidation in the Mexico City Metropolitan Area (MCMA) during April 2003, Atmos. Chem. Phys., 6, 2753-2765, 2006.

Wood, E. C., and Charest, J.: Chemical Amplification – Cavity Attenuated Phase Shift Spectrometer Measurements of Peroxy Radicals, Anal. Chem., 86, 10266-10273, 2014.